

Optical analysis of an 80-W light-emitting-diode street lamp

Kai Wang

Wuhan National Laboratory for Optoelectronics
Division of MOEMS
Wuhan, China, 430074
and
Huazhong University of Science & Technology
School of Optoelectronics Science and
Engineering
Wuhan, China, 430074

Xiaobing Luo

Wuhan National Laboratory for Optoelectronics
Division of MOEMS
Wuhan, China, 430074
and
Huazhong University of Science & Technology
School of Energy and Power Engineering
Wuhan, China, 430074

Zongyuan Liu

Bo Zhou

Zhiyin Gan

Wuhan National Laboratory for Optoelectronics
Division of MOEMS
Wuhan, China, 430074
and
Huazhong University of Science & Technology
School of Mechanical Engineering
Institute for Microsystems
Wuhan, China, 430074

Sheng Liu

Wuhan National Laboratory for Optoelectronics
Division of MOEMS
Wuhan, China, 430074
and
Huazhong University of Science & Technology
School of Mechanical Engineering
Institute for Microsystems
Wuhan, China, 430074
and
Huazhong University of Science & Technology
School of Optoelectronics Science and
Engineering
Wuhan, China, 430074
E-mail: shengliu63@yahoo.com

1 Introduction

Theoretically, the light-emitting diode (LED) has many advantages, such as high efficiency, good reliability, long life, variable color, and low power consumption. Recently, the LED has begun to play an important role in many applications.¹ Typical applications include backlighting for

Abstract. Optical analysis is critical to the evaluation of a light-emitting diode (LED) street lamp, especially when the lamp is still in its early stage of development and applications and when optimization is needed for making use of unique characteristics of LEDs. In this study, optical analysis of an 80-W LED street lamp was conducted. Experimental research on such a lamp was first undertaken. The results demonstrated that the average illumination was about 8.25 lx and the total uniformity was 0.364 for a 20-m-long and 10-m-wide test area at a height of 8 m, which is acceptable for the current standard for a submain road. Numerical simulation was also conducted; the feasibility of the numerical model was proven by comparison of the simulations with the experimental data, which will be used for future optimization study and other novel designs of the optical system of street lamps. Through the simulations and the corresponding analysis, it was found that the tested 80-W LED street lamp had reasonable performance in average illumination, but multiple shadows existed, which would need to be removed in future designs. Improvements are suggested to reduce the number of optical elements, to reduce the lamp's volume, and to enhance the illumination performance. Two design methods for LED street lamps are summarized, based on the optical analysis. © 2008 Society of Photo-Optical Instrumentation Engineers. [DOI: 10.1117/1.2835010]

Subject terms: light-emitting diode; LED street lamp; light distribution curve; optical modeling; numerical simulation.

Paper 070316R received Apr. 8, 2007; revised manuscript received Aug. 16, 2007; accepted for publication Aug. 16, 2007; published online Jan. 29, 2008.

cell phones and other LCD displays, interior and exterior automotive lighting (including headlights), large signs and displays, signals, and illumination. LEDs will soon be used in general lighting, which consumes a large proportion of the total energy all over the world. An expectation about the high-power LED is that it will be the dominant lighting technology by 2025.² Should that goal come to fruition, then up to 40 gigawatts a year could be saved in the USA

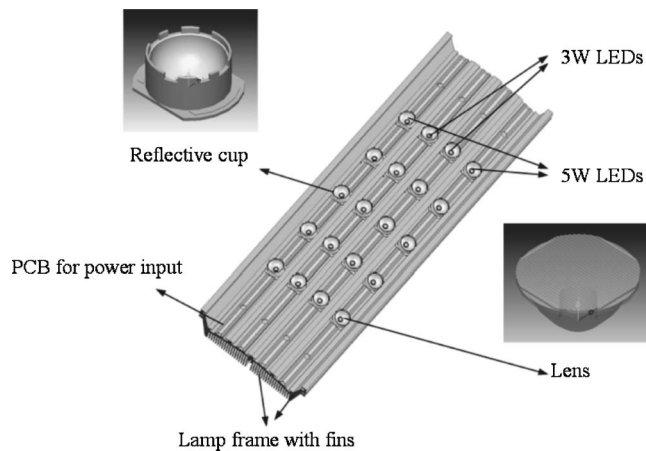


Fig. 1 Schematic diagram of the 80-W LED street lamp.

alone. It is generally believed that the LED can be widely used for general lighting in the USA. In China, however with the push of the government for more energy saving, the LED may be used ever earlier. The estimation by Chinese authorities is that if LED dominates the general lighting market in 2010, one-third of the present power consumption will be saved, which will greatly ameliorate the energy situation in China.

One typical LED general lighting product is the LED street lamp. It is estimated the need for new street lamps is about 380 million in China alone, not including the ones to be replaced. For modern LED street lamps, optical extraction and thermal management are two critical factors for high performance. Compared to the conventional lighting systems in use, which count on reflective surfaces to project the light onto the surface of the street, LED chips are unique in their small size, their nearly two-dimensional shapes, and the possibility of using large numbers in an array. The resulting direct lighting characteristics, together with the possibility of various designs of reflectors and lens systems, could significantly enhance their optical performance. In fact, a presentation by Philips Lighting showed that a single-chip LED light source can have an optical conversion efficiency of 70% to 90%, as compared to 40% to 70% for a bulb-type light source.³ Although these facts are useful for the street lamp design, the actual design of a LED street lamp can be complex and challenging. To our best knowledge, although there have been a few commercial announcements of street lamps in development,^{4,5} there has been no published analysis of the optical performance of any LED street lamp that has been developed or under development. It is believed that the lack of publications is due to the highly proprietary nature of such devices.

In order to promote the wide applications of the general lighting in general and street lighting in particular, it is essential to conduct an analysis of the optical performance of some newly developed street lamps, as compared to certain standards currently in use for conventional street lighting.⁶ This paper focuses on the optical analysis for an 80-W street lamp recently in trial use. It presents the problem statement, physical and numerical modeling, experi-

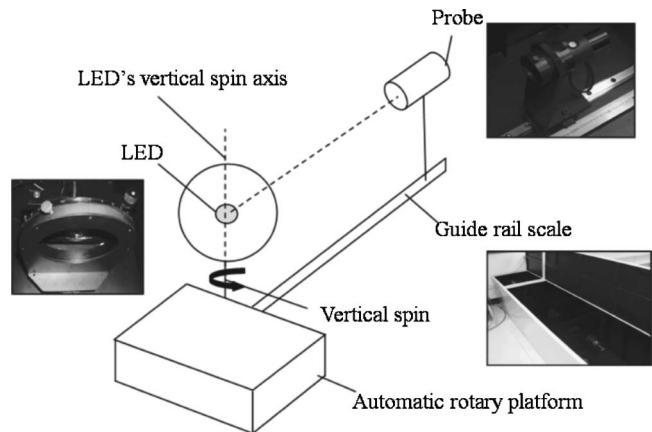


Fig. 2 Schematic diagram of Everfine GO1900L light distribution curve tester.

mental work, and comparisons. The results are discussed in terms of the advantages and drawbacks of this design, and suggestions are provided.

2 Problem Statement

Shown in the Fig. 1 is a schematic of the street lamp, with power consumption 80 W and with LED chips distributed on the surface of the substrate and the heat sink. The lamp is mainly composed of four parts: 20 high-power LEDs, 20 reflective cups and lenses, a lamp frame with fins, and four slim printed circuit boards (PCBs) for the power input of the LEDs. The lamp frame consists of an aluminum base and fins, which are integrated to save fabrication cost. The 20 high-power LEDs are directly bonded onto the aluminum base, to reduce the thermal resistance. They are distributed on the aluminum base in four rows, with the chips in the inner two rows consisting of LEDs of 3-W power, and the other two rows of LEDs of 5-W power. The reflective cups and lenses are placed on the LEDs and used for controlling the light rays. The four slim PCBs are located on the aluminum base and used for providing power input for the four rows of LEDs. The objectives of this research are (1) to provide an optical analysis of the developed design, (2) to find out the possible flaws in design as compared to the design standards for the specific applications, and (3) to come up with possible improvements.

3 Optics Experiments and Results

3.1 Physical Modeling of the LED Module's Optics

To analyze the effect of different optical elements on the lamp's total illumination performance, light distribution curves of a single base LED and an LED with a reflector or a lens were tested with an Everfine GO1900L light distribution curve tester, shown in Fig. 2, under the same drive voltage (3.2 V) and drive current (0.25 A).

In the curve tester, testing was realized by rotating the LED's vertical spin axis, which passed through the LED's optical center, and keeping the probe at rest, because that procedure could be made equivalent to the probe circumrotating on a spherical surface at a certain distance from the

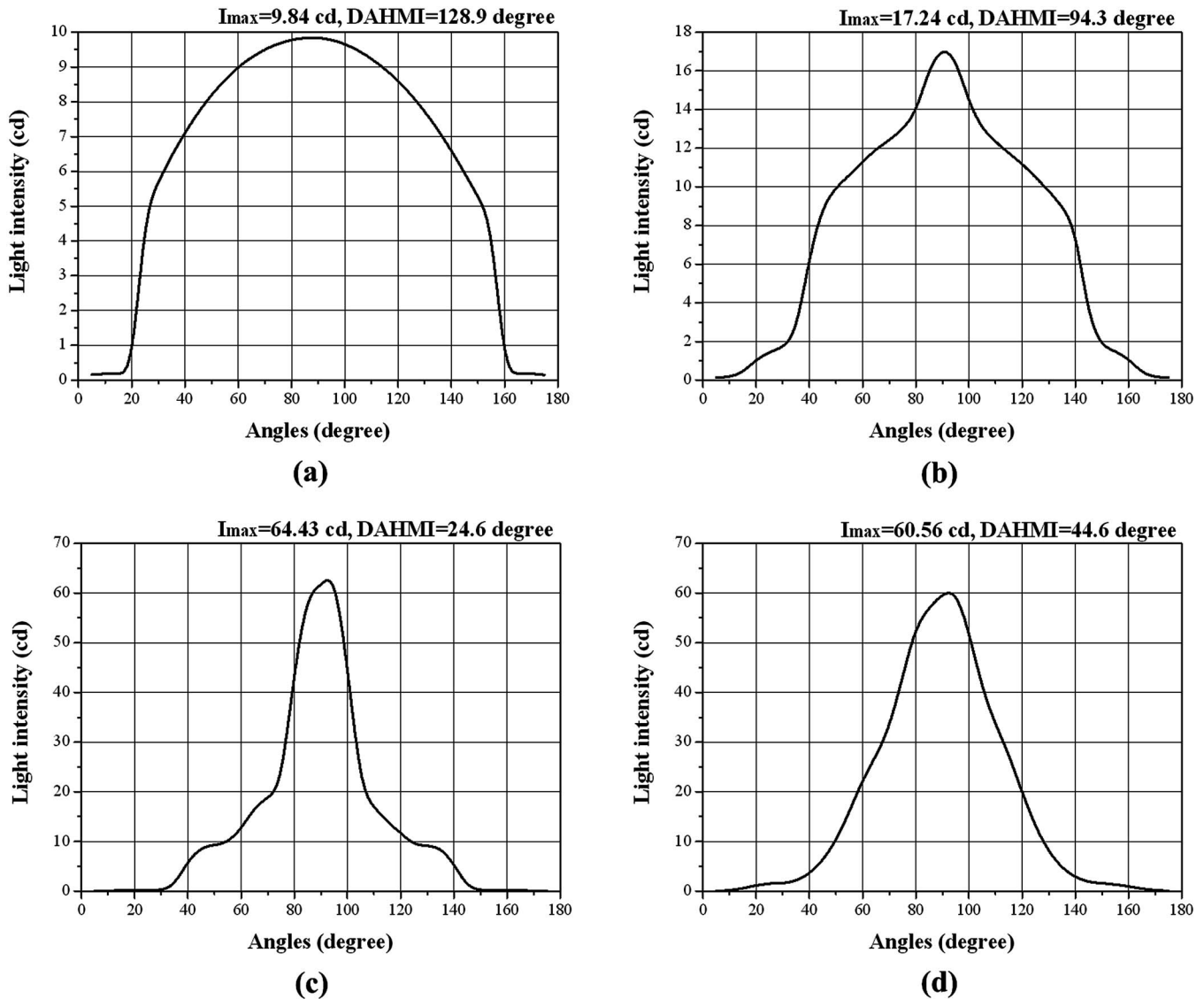


Fig. 3 Light distribution curves for a single LED; (a) bare; (b) with an unplated plastic reflective cup; (c) with an aluminum-plated reflective cup; and (d) with a lens and an aluminum-plated reflective cup.

test LED. According to the principles of photometry⁷ the relationship between illuminance and luminous intensity is expressed as

$$E = \frac{I \cos \theta}{d^2}, \tag{1}$$

where E is the illuminance, I is the luminous intensity, d is the distance between source and illuminated surface, and θ is the angle between the direction of the tested source beam and the normal direction to the surface. In this test system, the value of θ always is zero and $\cos \theta$ is one. Therefore, Eq. (1) can be simplified to

$$E = \frac{I}{d^2}, \tag{2}$$

resulting in

$$I = Ed^2. \tag{3}$$

The illuminance E can be measured by an illuminance meter in the tester, and the distance d can be measured by the guide rail scale at the bottom of the dark box. Therefore, the luminous intensity I can be calculated by Eq. (3).

The light distribution of a single base LED source [Fig. 3(a)] is approximately Lambertian. Because of the converging effect of the lens above LED chip, the luminous intensity decreases faster and the light distribution curve becomes mismatched to the cosine curve of the Lambertian distribution when the test angle is more than about 70 deg. The maximal intensity is 9.84 cd and the divergence angle of half-maximal intensity (DAHMI) is 128.9 deg. The LED luminous intensity distribution changes a lot [Fig. 3(b)] on placing a plastic reflective cup without aluminum film on the LED. The inner face of the reflective cup consists of two half spheres, which have a strong converging effect on

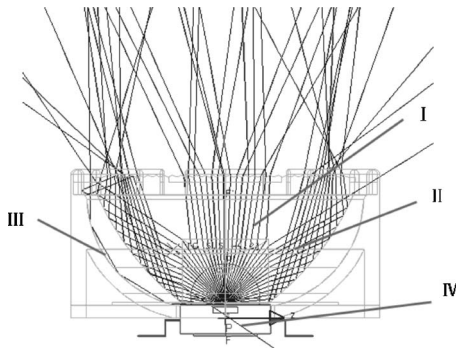


Fig. 4 Trace of the light rays emitted from the LED module.

light and turn the light distribution curve into a diamond shape. The maximal intensity increases to 17.24 cd and the DAHMI decreases to 94.3 deg. On changing the reflective cup to one with both sides aluminum-plated, the exit light becomes much more convergent, and more than 50% of the light is confined within a 30 deg divergence angle because of the reduction of scattering and absorption at the aluminum-plated inner surface. The maximal luminous intensity increases to 64.43 cd, and the DAHMI decreases to 24.6 deg [Fig. 3(c)]. On the basis of five tests, it is found that the maximal intensity does not appear to be at the center of light distribution curve, but slightly off, which may be caused by the asymmetric edge bulges of the reflective cup.

Although the convergence of exiting light increases after changing the plastic reflective cup to an aluminum-plated one, it is unnecessary for street illumination. It may in fact be too convergent, leading to alternating bright and dark patches on the street, which will reduce the uniformity, increase the probability of multiple shadows, and make pedestrians and or drivers uncomfortable. Therefore, in this street lamp design, there is a lens (Fig. 1) with a special structure on the LED module, which will control the direction of the light and increase the uniformity of street illumination. There are two special features of the lens: (1) a triangular-prism array covers the surface of the lens, with each prism's apex angle equal to 120 deg, which will di-

verge light within a certain angle and make the exit light much more uniform; (2) there is a small convex region at the bottom of the lens, which will confine the central light propagation direction and increase the luminous intensity at the center of the LED module.

The light emitted from the LED source can be approximately divided into four parts (Fig. 4):

1. The light rays I, propagating within the region of ± 25 deg from the center line, propagate almost vertically through the converging effect of the small convex lens region. After being refracted by the triangular-prism array, the exit light's divergence angle becomes about 35 deg. Rays I mainly make up the luminous energy distributed in the central region.
2. The main part of the light that is away from center line by more than 25 deg is refracted into the lens at the surface of the concave hole at the bottom. When these light rays (II) propagate in the lens, total internal reflection occurs at the inner surface of the lens. Then these rays are refracted out of the LED module by the triangular-prism array on the lens surface.
3. A minority of light rays (III) do not undergo total reflection because of their smaller incidence angle; they are reflected at the inner surface of the reflective cup by the aluminum film.
4. Even less light (IV) undergoes several reflections between the lens and the reflector before being absorbed by the LED module.

Therefore, the light emitted from the LED source is mainly distributed in the region around the vertical direction and propagated forward within a small divergence angle after being reflected and being refracted by the lens and reflective cup together. The maximal luminous intensity is high as 60.5 cd and about 70% of the light is contained within a 44.6 deg divergence angle [Fig. 3(d)].

There are two main advantages of a lens with this special structure. One is that the light rays diverge within a certain angle after going through the lens without the help of a large reflective cup, which simplifies the three-dimensional structure and reduces the total volume of the street lamp. The other is that most light rays undergo total

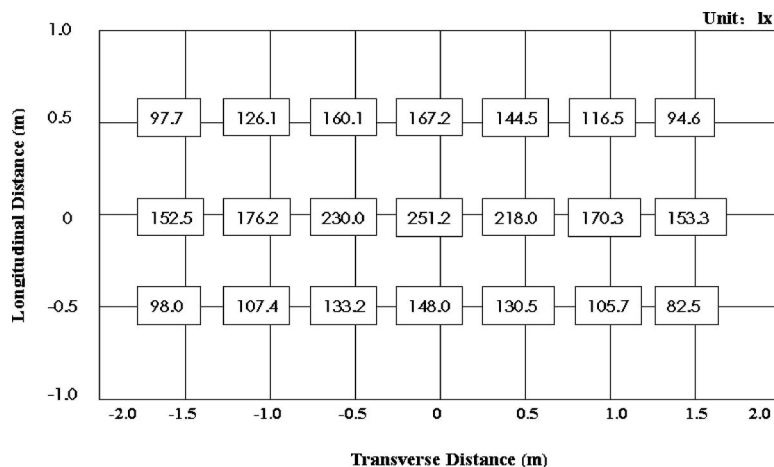


Fig. 5 Illuminance value at each mesh node.

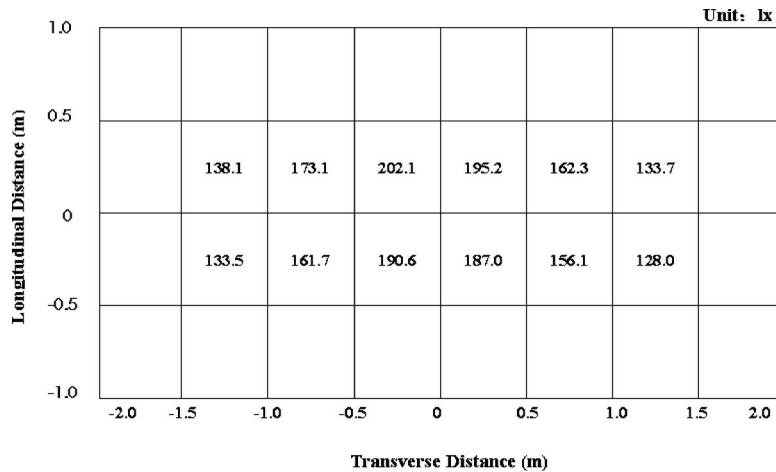


Fig. 6 Average illuminance value of each square in the mesh.

reflection at the inner surface of the lens without being reflected by the reflective cup, which will enhance the availability ratio of the exit light because the loss in total reflection is much less than that in reflection of the aluminum film.

3.2 Optical Experiments on the Whole Lamp

The overall illumination performance of the 80-W LED street lamp was also tested. The lamp was oriented in the vertical direction and irradiated a white wall, which was 3.4 meters away from the lamp. The wall was divided into a mesh of 32 squares, each 0.5 wide and 0.5 m high. The illuminance value at each mesh node was measured by an illuminance meter (Fig. 5). The equation to calculate the average illuminance of a certain square is:⁸

$$E_{av} = \frac{1}{4} \sum_{i=1}^4 E_i, \tag{4}$$

where E_{av} (lx) is the average illuminance value, and E_i (lx) is the illuminance value at one corner of the square. The average illuminance value of each square was calculated and is shown in Fig. 6.

When testing the lamp, it was found that multiple shadows were obvious on the white wall, which might be caused by the small number (only 20) of LED modules, the wide space between modules, and too small a distance between the lamp and the wall. Because the lamp was too close to the wall, an object's shadows, which appeared through irradiation by the LED modules, did not superpose completely with each other, which resulted in multiple

Table 1 Comparisons of road illumination performance between experimental data and the standard for sub main roads in China.

	Average illuminance (lx)	Overall uniformity
80-W LED street lamp	8.25	0.364
Standard for submain road	8.0	0.35

shadows. It can be found from Fig. 7 that the farther the lamp is from the wall, the fewer multiple shadows will be observed.

The illuminance distribution of the lamp used in an outdoor environment was measured. The distance between the lamp and the test area, which was 31 m long and 10 m wide, was 8 m and the elevation angle was 30 deg. The measured results are shown in Fig. 8.

The equation to calculate the total luminous flux Φ (lm) is as follows:

$$\Phi = \sum_{i=1}^n E_i M_i, \tag{5}$$

where E_i (lx) is the average illuminance of each square of the the test mesh, M_i (m²) is the area of each test mesh, and n is the total number of squares. The total luminous flux of one LED lamp, calculated by Eq. (5), is as high as 2080 lm. The calculation equations for the average illuminance (E_{av}) and total uniformity (U_0) are as follows:

$$E_{av} = \frac{\Phi}{\sum_{i=1}^n M_i}, \tag{6}$$

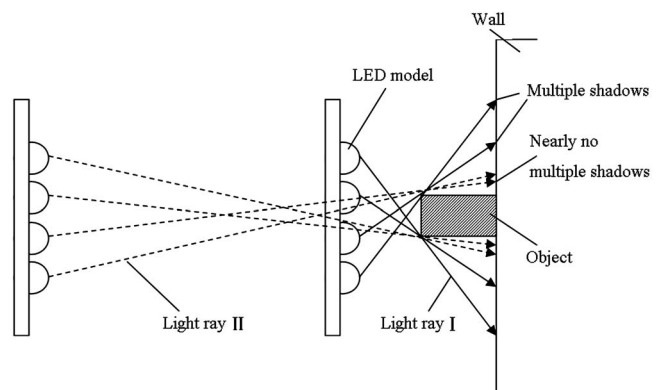


Fig. 7 Schematic of the cause of multiple shadows.

	15	14	13	12	11	10	9	8	7	6	5	4	3	2	1	0	1	2	3	4	5	6	7	8	9	10	11	12	13	14	15	16	
1	0.5	0.6	0.7	0.8	0.9	1.1	1.4	2.0	2.5	3.5	3.9	5.6	5.6	6.6	7.0	7.2	7.0	6.6	5.6	5.6	3.9	3.5	2.5	2.0	1.4	1.1	0.9	0.8	0.7	0.6	0.5	1	
2	0.5	0.6	0.7	1.0	1.0	1.4	1.9	2.7	3.7	5.3	6.7	10.1	10.4	13.9	14.2	15.4	14.2	13.9	10.4	10.1	6.7	5.3	3.7	2.7	1.9	1.4	1.0	1.0	0.7	0.6	0.5	2	
3	0.5	0.6	0.8	1.0	1.3	1.8	2.3	3.8	5.1	7.7	9.8	15.4	16.4	22.5	24.4	26.5	24.4	22.5	16.4	15.4	9.8	7.7	5.1	3.8	2.3	1.8	1.3	1.0	0.8	0.6	0.5	3	
4	0.6	0.7	1.0	1.2	1.6	2.1	2.9	4.6	6.3	10.0	13.4	20.0	23.5	29.0	33.6	34.2	33.6	29.0	23.5	20.0	13.4	10.0	6.3	4.6	2.9	2.1	1.6	1.2	1.0	0.7	0.6	4	
5	0.7	0.8	1.0	1.4	1.8	2.3	3.4	5.1	7.5	10.5	13.6	21.4	25.2	30.5	33.8	35.2	33.8	30.5	25.2	21.4	13.6	10.5	7.5	5.1	3.4	2.3	1.8	1.4	1.0	0.8	0.7	5	
6	0.7	0.9	1.1	1.4	1.9	2.5	3.6	5.0	7.7	10.0	14.0	18.8	22.3	24.2	26.2	27.6	26.2	24.2	22.3	18.8	14.0	10.0	7.7	5.0	3.6	2.5	1.9	1.4	1.1	0.9	0.7	6	
7	0.7	0.8	1.0	1.4	1.9	2.5	3.4	4.4	6.5	8.0	11.0	13.5	15.8	16.2	16.4	18.1	16.4	16.2	15.8	13.5	11.0	8.0	6.5	4.4	3.4	2.5	1.9	1.4	1.0	0.8	0.7	7	
8	0.7	0.8	1.0	1.3	1.8	2.3	2.8	3.6	4.8	5.9	8.0	8.9	10.2	10.7	10.6	11.6	10.6	10.7	10.2	8.9	8.0	5.9	4.8	3.6	2.8	2.3	1.8	1.3	1.0	0.8	0.7	8	
9	0.6	0.8	0.8	1.2	1.6	2.0	2.2	2.9	3.8	4.2	5.6	5.8	6.6	6.7	6.4	6.8	6.4	6.7	6.6	5.8	5.6	4.2	3.8	2.9	2.2	2.0	1.6	1.2	0.8	0.8	0.6	9	
10	0.6	0.7	0.8	1.2	1.4	1.6	2.0	2.4	3.0	3.2	4.0	4.0	4.5	4.5	4.4	4.5	4.4	4.5	4.5	4.0	4.0	3.2	3.0	2.4	2.0	1.6	1.4	1.2	0.8	0.7	0.6	10	
11																																11	
12																																	12
13																																	13
14																																	14
15	lux	30	30-25	25-20	20-15	15-10	10-5	5-3	3-1	1	1以下																					15	

Fig. 8 Illuminance distribution of the LED street lamp.

$$U_0 = \frac{E_{\min}}{E_{av}}, \tag{7}$$

where E_{\min} is the minimal average illuminance in the test area. Assume the distance between two LED street lamps is 20 m in actual street use and the whole illumination area is 20 m long and 10 m wide; then the minimal average illuminance can be estimated to be 3.0 lx from Fig. 8. Calculated by the preceding equations, the average illuminance is as high as 8.25 lx, and the overall uniformity is approximately 0.364, which are acceptable by the current standard for submain roads.⁶ (Table 1).

The lumen efficiency can be calculated by following equation:

$$\eta = \frac{\Phi}{P}, \tag{8}$$

where P (W) is the lamp's total power. Therefore, the lumen efficiency of the 80-W LED street lamp is about 26.0 lm/W. If the lumen efficiency can be increased to 47.3 lm/W, the lamp will be acceptable for the current standard for a main road in the same conditions.

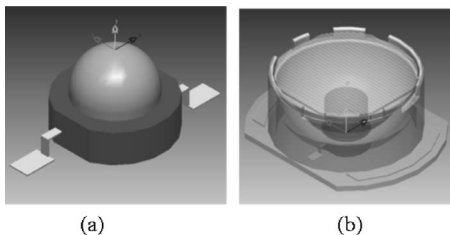


Fig. 9 Models of (a) single LED source and (b) single LED module.

4 Optical Simulation and Analysis of Results

4.1 Precise Optical Modeling for LED Modules

We used a commercial program to simulate the modules numerically by the widely used Monte Carlo ray tracing method. This method traces the desired number of rays, which can be thousands or even millions, from randomly

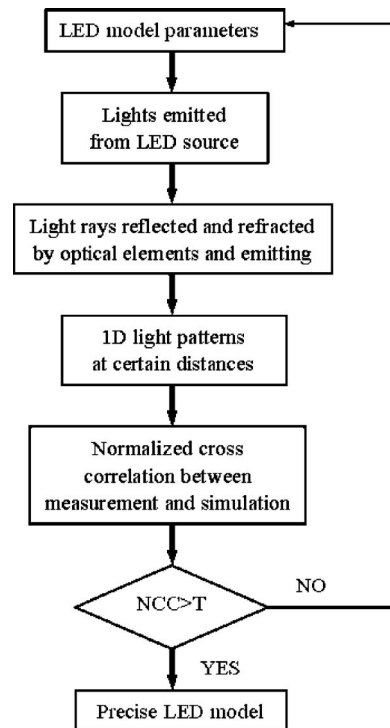


Fig. 10 Modeling algorithm for a LED model.

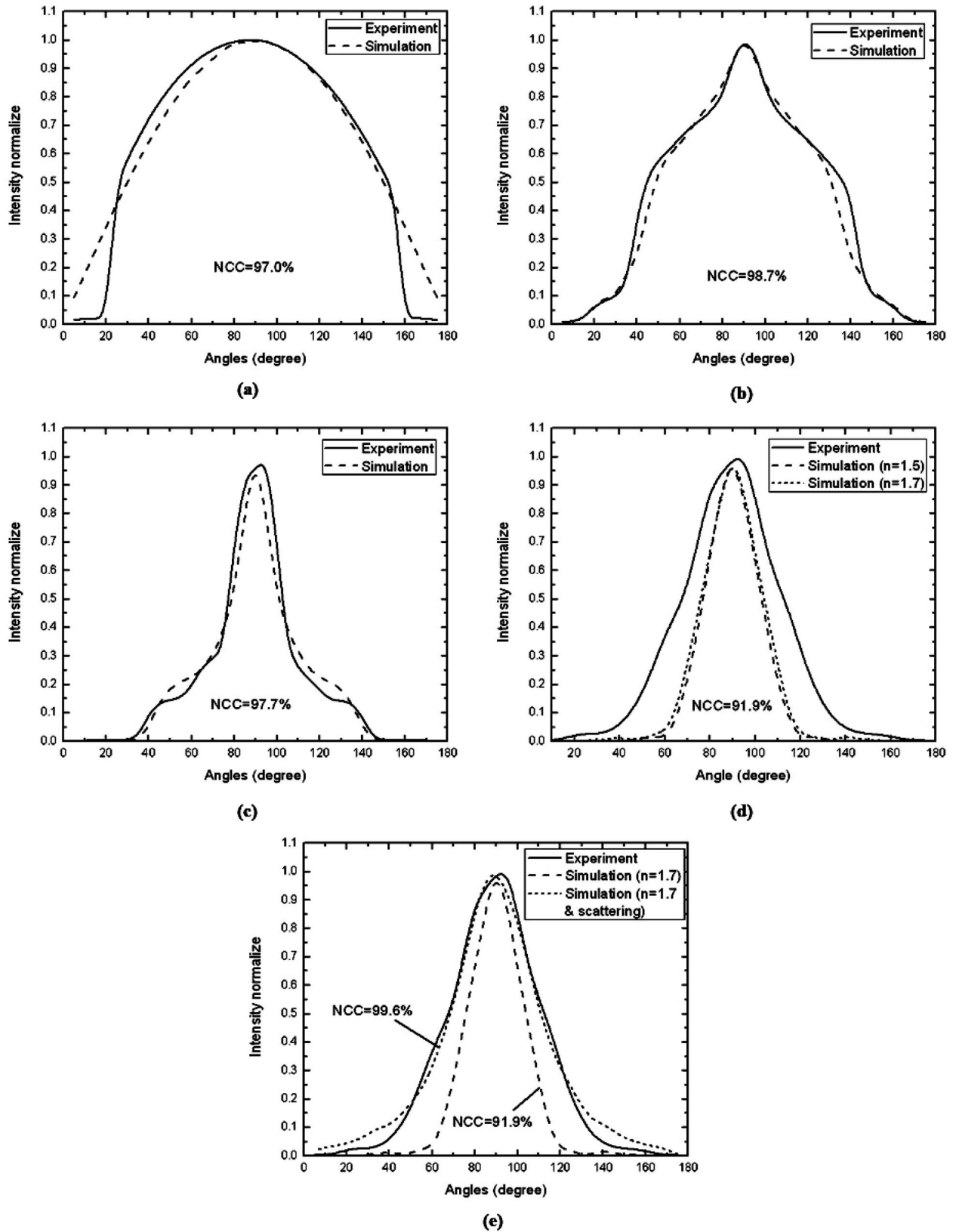


Fig. 11 Simulation light pattern versus experimental measurement for five samples: (a) single bare LED; (b) single LED with an unplated plastic reflective cup; (c) single LED with an aluminum-plated reflective cup; (d) single LED with a lens and an aluminum-plated reflective cup; (e) single LED with a lens (scattering) and an aluminum-plated reflective cup.

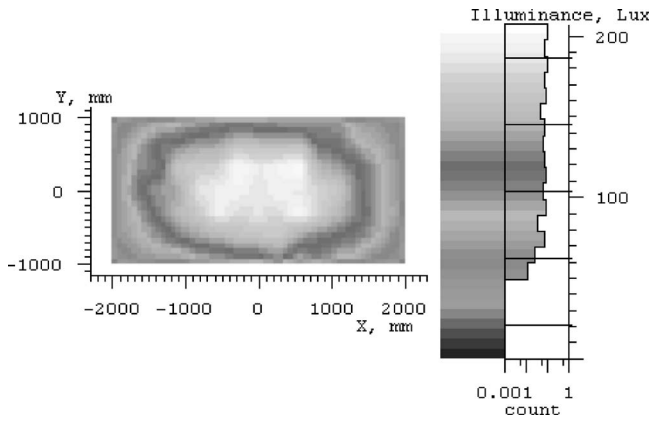


Fig. 12 Simulated illuminance distribution on a test area 4 m wide and 2 m high, 3.4 m away from the lamp.

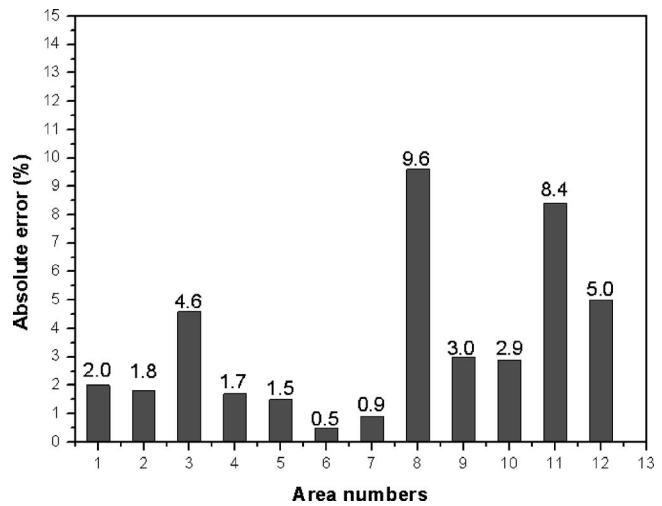


Fig. 14 Absolute error distribution of each test area.

selected points on the surface of, or within the volume of, the sources and into randomly selected angles in space. The selection of starting points and ray directions is based on probabilistic functions that describe emissive characteristics of light sources. Each ray starts with a specific amount of power, determined by its source’s characteristics; this power is then modified by the various surfaces hit by the ray in its path through the system. These rays are then collected on specified receiving surfaces for statistical analysis and graphical display.

Our LED module was simulated in four conditions, which were the same as the experimental conditions. We first made some simple measurements to determine the geometrical parameters of the LED module and estimated the material characteristic of the module (Fig. 9). We obtained the emitted rays by using Monte Carlo ray tracing from the LED source. Then one million rays were emitted from the LED source, and the luminous intensity distribution was obtained. To quantify the similarity between the simulation pattern and the experimental measurement, the normalized cross correlation⁹ (NCC) is applied. The NCC is written as

$$NCC = \frac{\sum_x (A_x - \bar{A})(B_x - \bar{B})}{\left[\sum_x (A_x - \bar{A})^2 \sum_x (B_x - \bar{B})^2 \right]^{1/2}}, \tag{9}$$

where A_x (B_x) is the simulation intensity or irradiance (the experimental) value of the and \bar{A} (\bar{B}) is the mean value of A (B), which is different from each other with the changing angle value along the x axis.

The modeling algorithm is summarized in Fig. 10, where the threshold value T of the NCC may vary from one case to another, depending on the application. If the NCC is below a threshold value, the parameters, such as the polymer material’s index and surface scattering characteristics, can be adjusted.

As shown in Fig. 11, the NCCs in the first three conditions are as high 96% or higher, which is acceptable for further simulation. In the fourth condition, the simulation light pattern mismatches the measurement badly, and the NCC is less than 92%, which is because the lens’s index

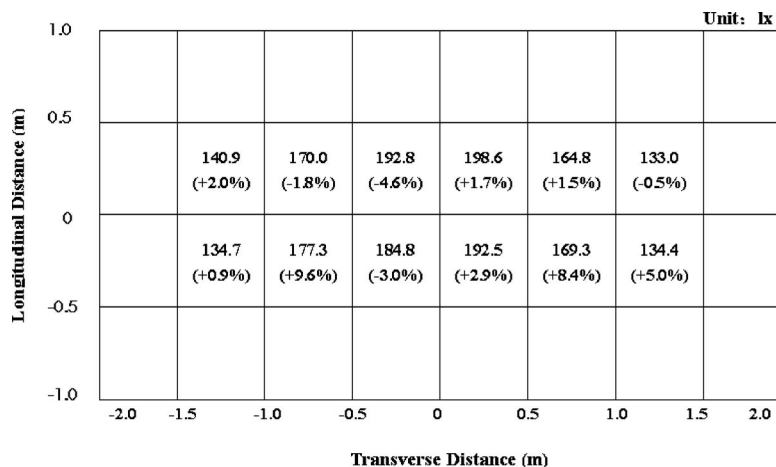
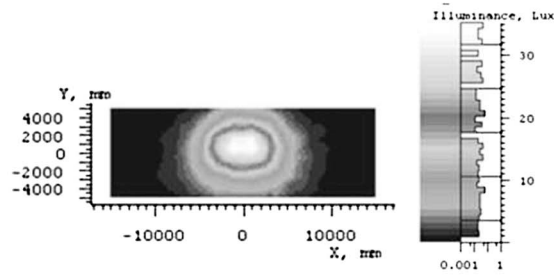


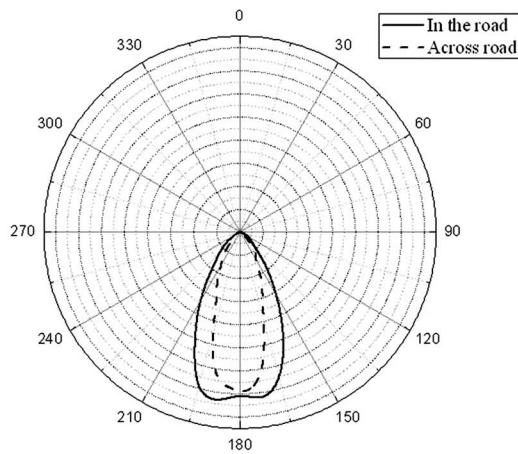
Fig. 13 Simulation average illuminance value and error in comparison with experiment.



(a)

	15	14	13	12	11	10	9	8	7	6	5	4	3	2	1	0	1	2	3	4	5	6	7	8	9	10	11	12	13	14	15	16	
1	0.1	0.2	0.2	0.3	0.4	0.4	0.5	0.9	0.9	1.6	2.2	3.7	6.2	7.7	8.7	8.9	8.3	8.0	5.8	3.8	2.1	1.5	1.0	0.7	0.6	0.4	0.4	0.2	0.2	0.2	0.1	1	
2	0.1	0.1	0.2	0.3	0.4	0.6	0.8	1.0	1.6	2.2	3.5	6.3	9.8	12.1	14.2	14.1	15.9	12.0	10.4	6.3	3.7	2.4	1.7	1.1	0.8	0.5	0.5	0.4	0.3	0.2	0.2	2	
3	0.1	0.2	0.2	0.4	0.5	0.8	0.9	1.4	2.4	3.6	5.8	10.2	15.4	18.8	21.4	22.0	21.0	18.4	15.0	9.5	5.9	3.7	2.4	1.4	1.1	0.8	0.5	0.4	0.4	0.2	0.2	3	
4	0.2	0.2	0.3	0.4	0.6	0.8	1.2	1.8	2.7	4.6	7.7	14.2	22.8	28.4	32.2	33.2	28.1	21.9	14.1	8.0	5.1	3.0	1.5	1.2	0.8	0.6	0.4	0.4	0.2	0.2	4		
5	0.2	0.3	0.2	0.4	0.7	0.9	1.4	2.0	3.4	5.6	9.4	15.4	23.7	29.9	34.2	34.3	31.8	29.7	22.6	15.9	9.5	5.7	3.4	1.8	1.1	0.8	0.5	0.4	0.4	0.2	0.2	5	
6	0.2	0.3	0.3	0.4	0.6	0.9	1.2	2.1	3.3	5.6	9.0	14.1	20.5	25.2	28.1	28.4	25.9	25.6	20.3	15.6	9.3	5.4	3.6	2.4	1.4	0.9	0.8	0.5	0.4	0.2	0.2	6	
7	0.3	0.3	0.4	0.5	0.6	0.8	1.3	1.9	3.3	4.7	8.2	13.8	19.6	25.6	29.7	29.5	26.5	20.5	15.5	10.1	12.4	8.2	4.7	3.1	2.0	1.5	0.8	0.6	0.5	0.4	0.3	0.2	7
8	0.2	0.2	0.4	0.4	0.6	1.0	1.4	1.9	2.8	4.1	6.0	9.0	10.6	11.5	12.7	12.4	12.1	11.8	10.1	8.1	6.2	4.0	2.8	1.6	1.2	0.9	0.5	0.4	0.3	0.3	0.2	8	
9	0.3	0.2	0.4	0.4	0.6	0.9	1.0	1.6	2.3	3.1	4.2	5.1	6.3	7.3	7.7	8.0	7.6	7.1	6.5	5.7	4.3	2.9	2.3	1.5	0.9	0.8	0.5	0.5	0.3	0.3	9		
10	0.2	0.2	0.3	0.4	0.5	0.6	0.9	1.1	1.6	2.3	3.1	3.8	4.3	4.8	5.0	4.8	5.0	4.6	4.2	3.9	3.2	2.3	1.6	1.2	0.8	0.7	0.6	0.3	0.4	0.2	0.2	10	
11																																11	
12																																	12
13																																	13
14																																	14
15		lux	30	20-25	25-20	20-15	15-10	10-5	5-3	3-1	1	lux																				15	

(b)



(c)

Fig. 15 Simulation illuminance distribution of the lamp in an outdoor environment: (a) overall illumination performance of the lamp; (b) average illuminance value of each square of the mesh; (c) light distribution curves.

and scattering characteristics were estimated approximately when the model was being built and are probably different from the actual ones. According to the modeling algorithm, we changed the lens's scattering characteristic and the value of the index, and adjusted them many times until the NCC was as large as 99% [Fig. 11(e)]. Thus, the precise optical modeling for single LED module is finished, and we can do further simulation for the whole LED lamp.

4.2 Optical Modeling for the Whole Lamp

The whole LED street lamp was also simulated. Figure 12 shows the simulation illuminance distribution on a test area 4 m wide and 2 m high that is 3.4 m away from the lamp. The receiver is divided into 2 mesh of 32 (8×4) squares, and the average illuminance value in each square is obtained during the simulation. As shown in Fig. 13 and Fig. 14, about 83% of the simulation errors are less than 5%,

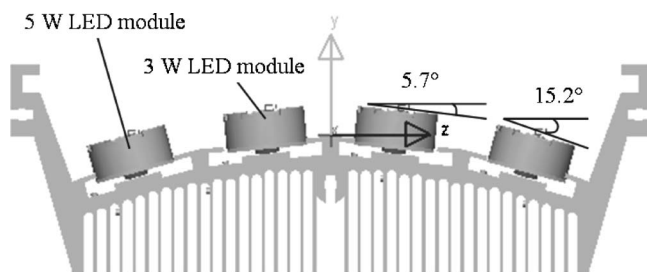


Fig. 16 Distribution of power and inclination angles of LED modules.

and the errors of the remaining 17% are around 10%, which is acceptable accuracy of simulation. In software, the average illuminance value is obtained by averaging all rays' luminous energy over the rectangular test area. This method is different from Eq. (4) and the software, which may have caused the error. In addition, differences in material parameters between the numerical model and the physical one, such as scattering and surface roughness, also may have caused the error.

The situation of the lamp used in an outdoor environment was also simulated. The position of the lamp and the size of the test area were the same as in the real situation. From the comparison of the simulated illuminance distribution [Fig. 15(b)] and the experimental one (Fig. 8), it can be found that the value for each square is similar to the experimental value in the central part of the area, but is quite dissimilar at the edges. This might be caused by scattering by the lamp's cover, surface roughness of the lamp's reflector, and inconsistency among LED modules. The lamp's cover is made of transparent plastic, and there are some patterns on its surface, which will scatter light and increase the luminous energy at large diverging angles. Roughness of the reflector surface also will scatter light. In addition, in the experiment we just measured one randomly chosen LED module's optical characteristics, and the remaining modules' optical characteristics were assumed the same. Actually, light patterns of some modules might be different from the measured one; if they had larger divergence angles, that might cause the simulation values near the edges to be much smaller than the measured ones.

4.3 Analysis of 3-D Structure Design

The power and inclination angles of LED modules are different between the inner two rows and the outer two rows. The inner LED modules' power is 3 W, and their inclination angle is ± 5.7 deg, the outer modules' is 5 W power and their inclination angle is ± 15.2 deg (Fig. 16). Here, the power distribution and inclination angles are specially designed to meet the current standard for a submain road. Because of the larger inclination angle as shown in Fig. 17, the distance from outer LED modules to the ground is longer than that of inner ones ($L_1 > L_2$). Therefore, in order to make the illuminance value at points A and D is similar to those at points B and C, so as to enhance the uniformity of road illumination, larger power will be needed for the outer LED modules. In addition, in order to expand the illumination area on the road surface, a properly enlarged inclination angle is needed for the outer LED modules.

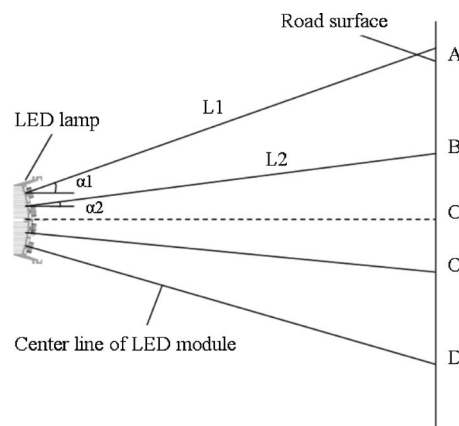


Fig. 17 Schematic of road illumination by the lamp.

However, if the inclination angle is too large, the irradiation on the road surface will not supply enough average illuminance, and (also will) result in obvious light pools on the road, which will reduce the illumination uniformity. Figure 18 shows the illuminance distribution on the road surface with different inclination angles of LED modules. It can be seen that the illumination performance becomes nonideal when the inclination angle is too large.

5 Improvements

Through simulations and corresponding analysis, it was found that the tested 80 W LED street lamp has reasonable average illumination performance, but multiple shadows exist, which might be prevented by reducing the spacing between LED modules or expanding the light distribution of each LED module. The more concentrated the LED modules are, the more concentrated the shadows will be. In the limit, the shadows are so close to each other that multiple shadows become indistinguishable.

To enhance the illumination performance, an asymmetric lens array could be used in future design, which will make the light distribution more nearly ideal and make better use of the lamps. To reduce the number of optical elements, we may note that lenses sometimes are unnecessary in the LED lamp design. The same illumination performance also can be obtained by special design of the reflectors: asymmetric reflector arrays, reflectors with novel 3-D distributions, etc. To reduce the whole lamp's volume, the array of LED modules might be replaced by one of LED chips if the thermal management could maintain a low junction temperature in the LED chips; then a corresponding microlens array, which also would reduce the volume, would be needed to control the light emitted from the LED chips. The improvements mentioned here could be used in further LED street lamp design to reduce the number of optical elements, to reduce the lamp's volume, and to enhance the illumination performance.

6 Design Methods for LED Street Lamps

Through the optical analysis of the 80-W LED lamp, two design methods for LED street lamps are presented. The two methods are respectively based on two different kinds of light sources: packaged LEDs and arrayed bare LED chips.

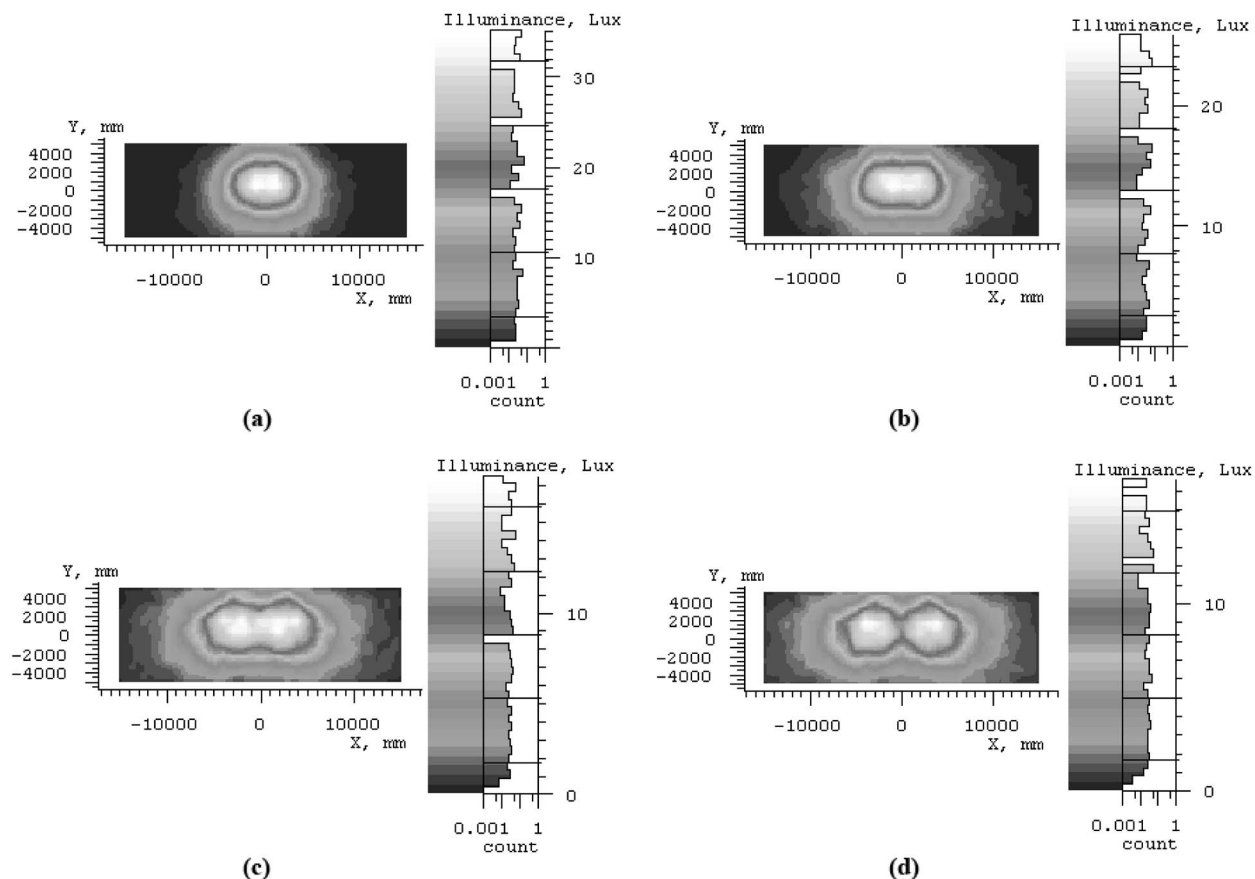


Fig. 18 Illuminance distribution for different inclination angles of LED modules: (a) 5.7 and 15.2 deg (inner rows and outer rows); (b) 5.7 and 30 deg; (c) 20 and 40 deg.; and (d) 30 and 40 deg.

When using packaged LEDs as light sources, the design process is shown in Fig. 19. First, we design corresponding lenses and reflectors to build a LED module. Then we observe the illumination performance on a certain test area after the light has gone through the optical elements. The pattern's size and brightness, as well as the LED module's light distribution curve, can be taken as the acceptance judgment criterion, depending on the application. If the LED module's illumination performance is not acceptable, we should modify the optical design until we obtain an acceptable result. Next, we design LED modules' 3-D structure and judge whether the overall illumination performance on the road surface is acceptable by comparing it with the standard. At each step mentioned, we should modify the 3-D structure if the design is unacceptable. Sometimes, we not only modify the 3-D structure, but also modify the LED module design again to satisfy the standard. Finally, a feasible LED street lamp design is finished.

When using arrayed bare LED chips as light sources, the design process is shown in Fig. 20. The process is similar to but simpler than the process shown in Fig. 19. The volume of this kind of LED lamp will be much smaller, because the LED chip arrays are very compact compared with LED modules. Therefore, this design method will reduce the LED lamp's volume, reduce its total cost, and extend its

application fields, and is likely to become the mainstream LED street lamp design method in the future.

7 Conclusions

In this study, optical analysis, including both models and experiments, of an 80-W LED street lamp was conducted. Experimental results demonstrated that the illumination design of this lamp was acceptable for the current standard for a submain road. If the lumen efficiency were increased to 47.3 lm/W, the lamp could be used on a main road. Numerical simulation was also provided, and the feasibility of the numerical model was proven by comparison of the simulations with the experimental data. Through the simulations and the corresponding analysis, it was found that the tested 80-W LED street lamp had reasonable performance in average illuminance, but multiple shadows existed, which might be avoided by reducing the spacing between LED modules or expanding the light distribution of each LED module. Improvements were provided to reduce the number of optical elements, to reduce lamp's volume and to enhance the illumination performance.

Two design methods for LED street lamps were summarized, based on optical analysis. The study of the 80-W

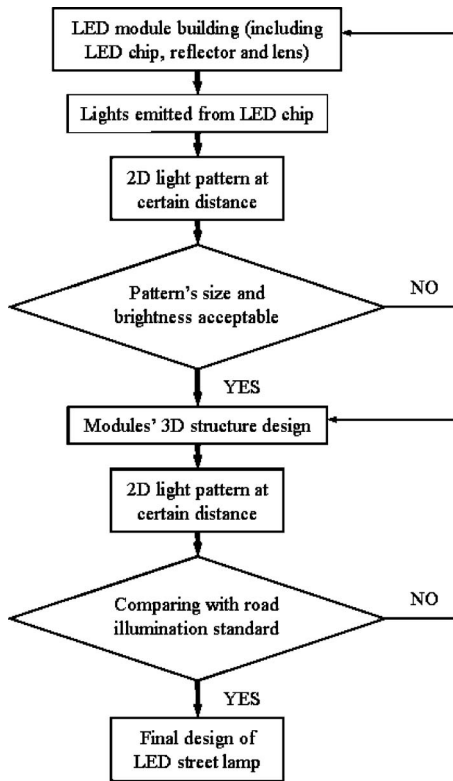


Fig. 19 Design process for LED street lamp using packaged LEDs as light source.

LED street lamp will be useful for future optimization study and for other novel designs of optical systems for street lamps.

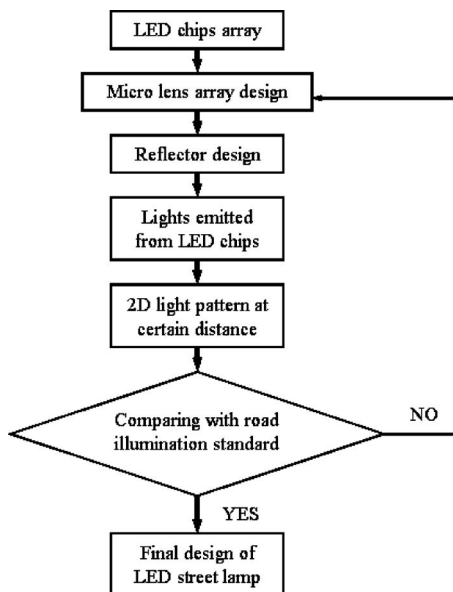


Fig. 20 Design process for LED street lamp using LED chips as light source.

Acknowledgments

The authors would like to thank Prof. Muqing Liu in the Light Source & Illuminating Engineering Department of Fudan University for his technical support with the lamps' illuminance distribution measurement.

References

1. M. Alan, "Solid state lighting—a world of expanding opportunities at LED 2002," *III-Vs Rev.* **16**(1), 30–33 (2003).
2. M. Alan, "Lighting: the progress & promise of LEDs," *III-Vs Rev.* **17**(4), 39–41 (2004).
3. *Philips Lighting Packaging Short Course Training Material*, Int. Conf. of Electronic Packaging Technology 2006 (2006).
4. C. Wei, S. Hui, D. Kongxian, and D. Youjan, "Optimal design of solar LED street lamp lighting system," *Zhongshan Daxue Xuebao/Acta Sci. Natur. Univ. Sunyatseni* **44** (Suppl. 2), 95–98 (Nov. 2005).
5. Dave, "Philips LED street lamps," http://forevergeek.com/news/philips_led_street_lamps.php.
6. China Academy of Building Research, *Standard of City Road Illumination Design CJJ445-91*, pp. 1–3, China Architecture & Building Press, Beijing (1996).
7. North America Illumination Association, *IES Illumination Basic Tutorial* (transl.), pp. 21–25, China Light Industry Press, Beijing (1984).
8. W. Jianping, D. Yuntang, and Q. Gongquan, *Road Illumination*, pp. 145–147, Fudan Univ. Press, Shanghai (2005).
9. C.-C. Sun, T.-X. Lee, S.-H. Ma, Y.-L. Lee, and S.-M. Huand, "Precise optical modeling for LED lighting verified by cross correlation in the midfield region," *Opt. Lett.* **31**(14), 2193–2195 (2006).



Kai Wang is a PhD candidate student in Wuhan National Laboratory for Optoelectronics. He received his BS degree in optical information science and technology from Huazhong University of Science and Technology, Wuhan, China, in 2006. Now his research interests include LED optical design and LED chip structure design.



Xiaobing Luo is a professor at Huazhong University of Science and Technology (HUST), Wuhan, China. He works in the School of Energy and Power Engineering and Wuhan National Laboratory for Optoelectronics at HUST. He received his PhD in 2002 from Tsinghua University, China. His main research interests are heat and mass transfer, LEDs, microfluidics, MEMS, sensors, and actuators. He has published more than 30 papers, and applied for or been granted 23 patents in the USA, Korea, Japan, Europe and China.



Zongyuan Liu is a PhD candidate student in Wuhan National Laboratory for Optoelectronics. He received his BS degree in mechanical design and manufacture and automation from Huazhong University of Science and Technology, Wuhan, China, in 2006. Now his research interests include LED packaging and LED module structure design.



Bo Zhou is a master's student in Wuhan National Laboratory for Optoelectronics. He received his BS degree in the Department of Mechanical Manufacturing and Automation, School of Mechanical Science and Engineering, Huazhong University of Science and Technology, Wuhan, China, in 2005. Now his research interests include LED packaging technology and optical design.



Sheng Liu is a special professor, the director of the Institute of Microsystems, and the director of the MOEMS Division at Wuhan National Laboratory for Optoelectronics, Huazhong University of Science and Technology, Wuhan, China. He obtained his PhD from Stanford University in 1992. His main research interests are LED, MEMS, IC packaging, mechanics, and sensors. He has published more than 200 technical articles and filed more than 50 patents.



Zhiyin Gan is an associate professor at Huazhong University of Science and Technology (HUST), Wuhan, China. He received his MS degree from Beijing Polytechnic University. His research interests are optoelectronics hybrid integration technology, and design and manufacturing methods for high-speed optically active and passive components.